

# **Repeated fluid expulsion through sub-seabed chimneys offshore Norway in response to glacial cycles**

Andreia Plaza-Faverola, Stefan Bünz and Jürgen Mienert

**Department of Geology, Dramsveien 201, University of Tromsø, Norway**

## **Abstract**

Focused fluid flow through sub-seabed sediments is a common phenomenon on continental margins worldwide. However, the governing controls and timing of this fluid release has been difficult to understand, in particular, for fluid flow features buried beneath sub-surface sediments. A link between fluid flow activity, ensuing pockmark formation and the last glacial maximum has been hypothesized on the formerly glaciated Norwegian Margin. New high-resolution P-Cable 3D seismic data from the Nyegga area on the mid-Norwegian margin reveal at least two more periods of fluid expulsion from sub-seabed sediments. The 3D seismic data show depositional patterns within chimney features, expressed as truncations of seismic horizons against the flanks of the chimneys. The truncations are interpreted, by analogy with present day observations, as evidence for buried carbonate mounds and/or sediment wash-out during formation of pockmarks in the past. The truncations are, hence, an indicator and a chronological marker for fluid expulsion in the past. The classification of chimneys results in three major groups: (1) Chimneys that have been formed and consecutively reactivated one or two times during the last 200 ka and that have a fluid flow expression at the present seafloor; (2) Chimneys that are approx. 125-160 ka old without any associated fluid-flow expression at the present day seafloor; (3) Chimneys with no stratigraphical evidence for reactivation formed after the last glacial maximum (18-25 ka). The observations suggest that each activity period was likely related to the last stages of Elsterian, Saalian and Weichselian glaciations. The emplacement of thick sequences of glacial debris flow deposits during these maximum stages most likely caused rapid increase in overpressure and subsequently the formation of focused fluid flow features piercing through sediments of the Naust formation at Nyegga.

**Keywords:** Nyegga, chimneys, fluid flow, 3D seismic, P-Cable, glacial cycles

## 1. Introduction

The continuous development of high-resolution acoustic seabed and sub-seabed mapping technology has led to worldwide discoveries of fluid escape-related features, such as pockmarks, mounds, mud volcanoes, chimneys and gas hydrate provinces (e.g. Barber et al., 1986; Foucher, 2009; Hovland and Judd, 1988; King and Maclean, 1970; Kopf, 1999; Kopf, 2002; Rise et al., 1999). These discoveries increasingly stimulate the interest of scientists and offshore industry for a better understanding of geological processes that control the migration of fluids from subsurface sediments to the seabed and into the water column, and possibly to the atmosphere. Particularly, the release of methane, a greenhouse gas, from shallow gas-hydrate bearing sediments is believed to have implications in climate change (e.g. Dickens, 2002; Kennett et al., 2003; Kvenvolden, 1993; Leggett, 1990; MacDonald, 1990; Nisbet, 2002; Nisbet and Chappellaz, 2009). Gas hydrates are predominantly composed of methane (CH<sub>4</sub>) gas (Milkov et al., 2003). They form in marine sediments when gas saturates pore water under appropriate pressure, temperature and salinity conditions within what is known as the gas hydrate stability zone (GHSZ) (Clennell et al., 1999; Milkov et al., 2003; Xu and Ruppel, 1999).

Fluid escape features are often recognized as columnar zones of seismic blanking and discontinuous reflections in seismic records. These features are commonly known as gas chimneys (e.g. Hustoft et al., 2010) or pipes (e.g. Moss and Cartwright, 2010). Chimneys or pipes have been largely described at many sites worldwide and are the result of focused fluid flow through sedimentary successions (Cartwright et al., 2007; Hustoft et al., 2010; Loseth et al., 2009). A common observation among authors is that pipes and chimneys are characterized by upward bending of seismic reflectors at their interiors within the GHSZ (Fig. 2A). In general there is common agreement in that these pull-up reflections are partially explained as velocity effects caused by high velocity material, i.e. large gas hydrate accumulations (tens of meters) and smaller carbonate accumulations emplaced in the conduits (e.g. Plaza-Faverola et al., 2010b). However, also true sediment deformation (doming) caused by the buoyancy of moving gasses at early stages of chimney formation is expected (Cathles et al., 2010; Judd and Hovland, 2007, pp 228). In addition, carbonate precipitations and sediment wash-out during fluid expulsions result in real morphological features (e.g. Judd and Hovland, 2007).

In Nyegga, offshore Norway (Fig. 1), many chimneys connect to pockmarks or mounds at the present-day seafloor where authigenic carbonates document the micro-seepage of dominantly light hydrocarbon with a mixture of heavier hydrocarbons (Hovland and Svensen, 2006; Hovland et al., 2005; Mazzini et al., 2006; Paull et al., 2008; Vaular et al., 2010). Light hydrocarbons may indicate gas-hydrate dissociation (Naehr et al., 2007). Bacteria mats (Hovland et al., 2005) suggest active micro seeping of methane. Shallow accumulations of gas hydrate (Akhmetzhanov et al., 2008; Vaular et al., 2010) also provide evidence for relatively recent fluid migration in Nyegga. Sizes and morphology of pockmarks in the region are well constrained (Hustoft et al., 2010).

Detailed seismic investigation of chimney-like features in Nyegga associated with the G11 pockmark (Jose et al., 2008) and the CNE03 pockmark (Plaza-Faverola et al., 2010b; Westbrook et al., 2008) shows that the two chimneys are currently filled with high velocity material, most likely gas hydrate, buffering and allowing the escape of methane to the water column. Hydrate concentrations at one investigated chimney was estimated to about 14 % of the total volume (Plaza-Faverola et al., 2010b) assuming predominantly fracture-filling models for the emplacement of gas hydrate (Jain and Juanes, 2009) in fine-grained shallow sediments at Nyegga (Berg et al., 2005; Rise et al., 2005).

Timing of fluid flow activity has been more difficult to constrain. Basin modeling (Hustoft et al., 2009) and AMS  $^{14}\text{C}$  dating methods of carbonate from pockmarks (Mazzini et al., 2006; Paull et al., 2008) suggested that a major period of fluid expulsion happened between 16-19 ka BP.

New high-resolution 3D seismic data allows us to identify structures and depositional patterns within the chimney and at its flanks that are not resolved on conventional 3D seismic data. These observations enhance the seismic characterization of chimneys in Nyegga and allow us to improve our understanding of chimney genesis and its timing. In this paper we have mapped and analyzed depositional patterns within chimney structures that can be linked to former periods of fluid expulsion. The timing of these periods show a clear relationship with the Elsterian, Saalian and Weichselian glaciations in the region corresponding to marine isotope stages (MIS) 10, 6 and 2 respectively (Hohbein and Cartwright, 2006; Jansen and Sjøholm, 1991; Rise et al., 2006; Sejrup et al., 2004).

## 2. Studied area

The Nyegga region is located on the mid-Norwegian continental margin at a water depth between 700-800 m, at the northern flank of the Storegga slide (Fig. 1).

The study encompasses sediments within the gas hydrate stability zone of the Naust Formation (Fig. 2). The Naust formation encompasses glacial-interglacial sediment deposits (Berg et al., 2005; Hjelstuen et al., 1999; Nygård et al., 2005). It consists of several 100 meters of debris flow deposits interbedded with thinner hemipelagic and contouritic sediment deposits (Bryn et al., 2005). In the Storegga region, hemipelagic and along slope contouritic sedimentation prevailed prior to shelf edge glaciations. During peak glaciations the ice sheet reached the shelf-edge, and the slope was dominated by glacial debris flow deposition (Rise et al., 2006).

The age of the Naust Formation is approximately 2.8-0 Ma (Rise et al., 2006). Sediment progradation from inner shelf towards the continental slope occurred at water depth between 500-1000 m during Naust time, considerably increasing the sedimentation rate compared to Eocene-Pliocene periods (Eidvin et al., 2000, Rise et al., 2005). This study focuses on the upper three Naust units (Fig. 2). Following the notation from Rise et al., (2006) it consist of Naust unit U (600-400 ka.), Naust unit S (400-200 ka) and Naust unit T (200-0 ka). The three units represent different stages between glacial and inter-glacial conditions (Berg et al., 2005).

Naust unit U consists of silty clay with variable content of sand and gravel and has a contouritic seismic character with interbedded cycles of glacial debris flows (Berg et al., 2005). The transition from Naust U to Naust S is from less to more coarse-grained and unsorted deposits (Berg et al., 2005). Naust unit S is typically characterised by contourite deposits that appear as climbing internal reflectors in seismic sections in the up-slope direction (Berg et al., 2005; Bryn et al., 2005). It also represents debris flow units that accumulated several hundred meters of sediments on top of the contourite sediments. The debris flows have a low permeability and create an effective seal for fluids. As a result, increases in excess pore pressure may occur within and beneath Naust unit S (Rise et al., 2006).

The uppermost unit, Naust T, is subdivided into subunits separated by the INT reflector representing the final Saalian ice sheet retreat at ~130ka (Berg et al., 2005). Beneath the INT reflector, Naust unit T consists of silty, sandy clay with shell fragments and larger clasts

(Berg et al., 2005). Above the INT reflector, Naust unit T is clay rich, with variable content of silt, sand and scatter gravel indicating glacial influence (Berg et al., 2005).

Bottom current activity has influenced the sedimentation along the mid Norwegian margin since mid-Miocene time and contourite drifts deposited during glacial-interglacial cycles. The contouritic infill appears as extensive homogenous layers with more brittle sediments compared to the glacial deposits, and represents sediment accumulation periods of approximately 100 ka (Bryn et al., 2005).

### **3. Data and methods**

In 2008, a R/V Jan Mayen cruise from the University of Tromsø (Bünz et al., 2008) acquired P-Cable high-resolution 3D seismic data at the Nyegga pockmark field (Fig. 1). The P-Cable seismic acquisition system (Petersen et al., 2010; Planke and Berndt, 2003) consists of an array of up to 16 streamers, each 25 m long with 8 recording channels. The streamers are connected to a cable that runs perpendicular to the vessel's steaming direction. This so-called cross cable is spread behind the vessel by two large trawl doors. The spacing of streamers along the cable is 15 m. However, due to the curvature of the cable, the distance between streamers is varying between 8-12 m. The seismic source was one GI (Generator-Injector) gun fired in true GI mode at 45/105 in<sup>3</sup> at a pressure of about 140 bars (Bünz et al., 2008). The 3D seismic data covers an area of 3x10 km<sup>2</sup>, at 10-15 km north of the northern sidewall of the Storegga Slide (Fig. 1). The dominant frequency of the seismic data is 80 Hz resulting in a vertical resolution of approximately 5 m.

The data was processed by DECO using RadExPro Plus software®. Geometry of the 3D seismic survey and navigation were processed on board. Final processing included static and tidal corrections, amplitude corrections for spherical divergence, stacking, bandpass filtering interpolation to fill trace-gaps and Stolt post-stack migration. The bin spacing of the seismic data is 6 m and sampling interval 1 ms. In general, the quality of the data is very good. However, some acquisition-related amplitude artifacts can clearly be differentiated from real geological features.

Seismic units were typified by the magnitude of lateral thickness changes, expressed in thickness maps, and by the type and distribution of dominant geological features such as iceberg ploughmarks and chimneys at the top and base reflectors of the units, expressed in root mean square (RMS) amplitude maps. RMS maps were calculated for amplitude samples within time windows of 15 ms in the non-migrated data set to use seismic diffractions at

chimney and ploughmark flanks as enhancers of investigated features. High amplitude diffractions along the flanks of iceberg features or against flanks of amplitude-attenuated-chimneys improve the isolation of the features facilitating the interpretation. Time thicknesses were converted to meters using P-wave interval velocities from Plaza-Faverola et al., (2010b).

Depositional patterns associated to the flanks and fronts of chimneys were investigated using attributes that enable to localize lateral changes in the properties of the seismic signal (i.e. number of zero crossing and signal loop duration). The implemented zero crossing attribute counted the number of zero crossing within the 12 ms time window covering the immediate signal period above the base of investigated stratigraphic units. The loop duration attribute identified lateral changes in the time lengths of the signal from the first to the second zero crossing point within a given time window.

## **4. Results**

### **4.1 Stratigraphic interpretation**

#### *Inter-stratigraphic units within the Nyegga GHSZ*

Thickness maps and RMS amplitude maps were used to characterize stratigraphic units within the GHSZ (Figs. 2, 3). We adopted the stratigraphic division and nomenclature of Plaza-Faverola et al., (2010b) where “L” stands for layer and “H” stands for horizon. Five units are described from bottom to top (Figs. 2, 3): L100, L70, L60, L50 and L30.

Unit L100 shows an average thickness of 55 m. The estimated depth of the GHSZ at the investigated Nyegga site lies within L100 (Bünz et al., 2003). A thickness increase of 15 m characterizes the north-west end of the unit (Fig. 2-F). It is due to a toe of a glacial debris flow deposit that progrades from the north-east reaching the north-west corner of the study area (Fig. 1). The seismic data show elongated, narrow (<50 m width) and curved lineations at the base of the unit (Fig. 3-G). They are often associated with small depressions (< 5m) and are interpreted as iceberg ploughmarks similar to those that occur widespread on the Norwegian shelf (Ottesen et al., 2005). Ploughmarks observed at this depth occasionally cross each other but generally follow a nearly north-south orientation (Fig. 3-G).

Units L70 and L60 are characterized by sediment thickness increases up to 8-10 m towards the west and south-east respectively (Fig. 2-D, E). These sediment thickness differences within the units may be related to the thickness difference (thicker towards the south) within the northward up-slope transported contourite deposits with material derived from the North-

sea Fan during intra glacial periods (Bryn et al., 2005). Ploughmarks are absent in units L60 and L70 (Fig. 3-E and F).

Unit L50 shows an average thickness of 30 m. In contrast to underlying units, the maximum sediment thickness increase observed is only 3 m towards the east (Fig. 2-C). Ploughmarks are characteristic features of this depositional unit (Fig. 2-C). They are 100-200 m wide and 5-10 m deep. Water depths of 660-700 m are estimated for L50 deposition time, according to sea-level curves (Dahlgren et al., 2002) and subsidence rates (Hjelstuen et al., 2005) reported from this area. Water depth and dimension of ploughmarks within L50 make them comparable to relict large icebergs (Clark et al., 1989) reported in the Arctic Ocean (e.g. Polyak et al., 2001) instead of modern iceberg ploughmarks generally seen at water depths shallower than 400 m (Lygren et al., 1997; Wadhams, 2000). The occurrence of ploughmarks above the BGHSZ, H50 (base of L50) and INT (top of L50) reflectors (Fig. 3-C, D, G) suggests a depositional environment of floating icebergs and confirm that intermittent glaciations with ice sheets reaching the shelf edge (Berg et al., 2005; Hjelstuen et al., 2005; Hohbein and Cartwright, 2006; Rise et al., 2005) affected the Pleistocene deposition in Nyegga. The lack of a significant sediment thickness increase but frequent ploughmarks makes unit L50 unique if compared to overlying and underlying units.

Unit L30 is comparable in character to units L60 and L70. It has a maximum thickness increase of 10 m towards the east (Fig. 2-B). Except for the ploughmarks at INT (base of unit L30, top of unit L50) they are absent within the unit (Fig. 3-A, B).

#### *Chrono-stratigraphy.*

The current study comprises sediments of the Plio-Pleistocene Naust formation, which encompasses sediments of the glacial-interglacial cycles. The stratigraphy for this formation has been well established (Hustoft et al., 2010; Rise et al., 2006) and was extended into the P-Cable 3D seismic volume (Fig. 4). In addition, approximate periods of glaciations (Berg et al., 2005), marine isotope stages (Hjelstuen et al., 2005) and age of Naust units and intra reflectors (Rise et al., 2006) established at Nyegga and nearby were included in the correlation.

The top of Naust U (Fig. 4) is a regional unconformity dated to be approximately 400 ka (Rise et al., 2006). It can be identified over the entire mid-Norwegian continental margin (Berg et al., 2005) facilitating the stratigraphical correlation in this study. The P-cable seismic data show that the top of Naust U lies between the present-day BGHSZ and the top of a high amplitude zone (HAZ) associated to a shallow gas reservoir in the region (Fig. 4) (e.g. Plaza-

Faverola et al., 2010a). Naust unit S (Fig. 4) represents the time interval from 400-200 ka (Rise et al., 2006) corresponding to MIS 8-10 (Hjelstuen et al., 2005) and it comprises the Elsterian glaciation (Berg et al., 2005).

The H50 reflector (base of L50 unit) (Fig. 4) may correspond to MIS 6, the end of the Saalian glaciation (Hjelstuen et al., 2005), which according to Dahlgren et al., (2002) corresponds to 128-186 ka. The INT reflector itself is interpreted to represent the final Saalian ice-sheet retreat (Berg et al., 2005). The age of INT is estimated to be 125-130 ka (Berg et al., 2005; Rise et al., 2006; Sejrup et al., 2004). Using 1.4 m/ka as sedimentation rate for the MIS 6 period (Hjelstuen et al., 2005) and 40 m as sedimentary thickness between INT and the base of L50 (Plaza-Faverola et al., 2010b), the estimated age for the base of L50 (H50 reflector) is approximately 160 ka. However, Hjelstuen et al. (2005) also report a sedimentation rate of 0.5 m/ka at the deposition time of the INT reflector (MIS 5e). Using this sedimentation rate the estimated age for H50 reflector is ~200 ka. As a result, the accurate age assignment for the H50 reflector is doubtful and has an uncertainty of ~40 ka. However, the presence of ploughmarks at the depth of the INT and H50 reflectors (Fig. 3-C, D) supports a correlation of L50 unit with the end of the Saalian glaciation (Fig. 4).

On the sedimentation-fluid flow model presented by Hustoft et al., (2009) the LGM (~25 ka) has been correlated with a reflector at ~ 25 mbsf. This LGM reflector corresponds with a comparable strong reflector at ca. 25-30 mbsf in the P-cable seismic data (Fig. 4). A more precise correlation of the LGM would require an age-dated sediment core, which is not available from the site.

## **4.2 Seismic expression of chimneys**

The seismic character of chimneys observed in the P-Cable 3D data is similar to chimneys typically described in other Nyegga sites and adjacent areas (e.g. Hustoft et al., 2010; Plaza-Faverola et al., 2010a; Fig. 2-A). They are characterized by pull-up reflections within the GHSZ, strong seismic blanking and strong diffractions associated with their flanks and fronts (Fig. 3-E). The chimney flanks correspond to the lateral termination of seismic blanking and up-bending of strata. Similarly, chimney fronts correspond to the vertical termination of the blanking zone and up-bended strata. The chimneys advance towards the seafloor but not all of them has a seafloor expression associated (Fig. 3-A).

In addition to these previously reported seismic characteristic of chimneys, detailed observation of the seismic response of each chimney imaged by the 3D P-Cable seismic data



allowed for the recognition of small scale truncations of seismic reflections against the flanks or fronts of some particular chimneys (Fig. 4-inset, 5, 6-A,E and 7).

#### **4.2.1 Seismic truncations**

By truncations we refer to arbitrary terminations of seismic reflections compared to continuous reflections (Fig. 6-I) corresponding to specific stratigraphic events during the time of sediment deposition. For simplicity, we will refer to the chimneys where seismic truncations are observed as truncated chimneys and equivalently, where seismic truncations are absent as non-truncated chimneys.

Fig. 5 shows the zero crossing and the loop duration maps at the base and top of L50 (H50 and INT reflectors respectively), where truncations are easily recognizable. A truncation causes a decrease in zero crossings of the seismic signal (Fig. 5-A) because it removes at least one full phase from the seismic signal, hence, also removing at least one zero crossing. Then again, loop duration increases because two phases with equal polarity merge thereby widening its composite phase. In contrast, maps associated with the base of unit L60 (Fig. 2-D) show no evidence for truncations (Fig. 5-E, F).

If these truncations were artefacts of data processing we would expect that they appeared systematically through the seismic volume at specific depths, at the location of every chimney or that they affected more than one consecutive reflection. Hence, the truncations are the result of some true geological process related to the formation of the chimneys.

The background number of zero-crossings is 3, which corresponds to parts of the INT and H50 maps where chimneys or ploughmarks are absent (Fig. 5-A and C). A drop to lower numbers of zero-crossing ( $< 3$ ) in adjacent seismic traces indicates truncation of a seismic reflection (arbitrary termination).

Most of the observed truncations against chimney flanks appear at the depth of H50 reflector (Fig. 5-C and D). A few chimneys present truncations at the depth of both INT and H50 reflectors. Some chimneys are considered to be non-truncated. Strong blanking hinders the recognition of continuation of the seismic reflectors (Fig. 6-F, G and H) and makes the classification of some chimneys difficult.

Taking into account differences in the truncation pattern together with the depth at which the chimney's fronts (termination of seismic blanking and up-bending of reflectors) are observed the chimneys can be sub-classified into 8 types (table 1). Five types belong to the truncated and three to the non-truncated chimneys.

#### **Truncated chimneys**

Type (a) chimneys (table 1) exhibit truncations at the depth of H50 reflector. No seismic blanking or doming of strata is observed above the truncated reflection (Fig. 6-A). This type of chimney is therefore considered to terminate at the depth of the truncations. Seafloor pockmarks or seismic indicators of continuous seepage towards the present-day seabed are also absent (Fig. 6-A). Not all the chimneys terminate at the H50 reflector or beneath it. Some chimneys with truncation at H50 terminate close to the present seafloor (type b). Most of them are associated with seafloor pockmarks (Fig. 6-B). Other chimneys with truncations are located at the flanks of ploughmarks (Fig. 6-C), which makes it difficult to judge the nature of the truncation. Only a few cases exist where the truncations are clearly recognized at the depth of both the H50 and INT reflectors (Fig. 6-D and E). In these cases the chimneys terminate again at the depth of INT reflector. That is, the front is within the L50 unit (between H50 and INT reflectors). While some of this chimney type lack a connection to pockmarks at the seafloor (Fig. 6-D) others do connect to characteristic pockmarks (Fig. 6-E).

#### **Non-truncated chimneys**

The remaining chimneys do not show any clear evidence for truncations. Non-truncated chimneys are significantly narrower than those showing truncations (Fig. 6-F, G and H). Some of them terminate (chimney fronts stop) at the depth of H50 without visible truncation (type f, table 1) but they may have a well develop pockmark associated (Fig. 6-F). Non-truncated chimneys may also terminate closer to the seafloor but without a continuation to a pockmark (Fig. 6-G). The last type (type h) shows non-truncated chimneys that penetrate to the seafloor and connect to a well defined pockmark (Fig. 6-H).

#### **4.2.2 Diameter variations of chimneys with depth**

In Nyegga chimneys terminate at different stratigraphical levels and present variations in their diameters with depth. The chimneys are clearly recognized in time-depth slices as circular to elliptical features associated with low RMS amplitude values (Fig. 3). The top of L50 marks a decrease in the number of chimneys progressing towards the seafloor (Fig. 3-D), i.e. from the number of chimneys mapped at the depth of H50 reflector approximately half appears preserving its diameter at shallower depths (Fig. 3). Some of the chimneys do not appear at all in shallower maps and some others are only represented by smaller amplitude anomalies. Clearly, the density of pockmarks (seafloor expression of chimneys) within the shallowest few tens of meters of sediments (Fig. 3-A) is less when compared to the density of chimneys at greater depths (Fig. 3).

The diameter of chimneys varies within the sedimentary column they pass through (e.g. type b, c and e chimneys). Some of these chimneys have narrower conduits (seismic blanking and doming of strata) above the truncated reflections (INT and H50) compared to conduits beneath them (Fig. 7).

Doming of the strata and seismic blanking, characterizing some of the truncated chimneys, stop at a few tens of meters beneath the present day seafloor or at the truncated reflections at H50 or INT (Fig. 6). Nevertheless some of these chimneys apparently connect to pockmarks or mounds at the seafloor (Fig. 6-C, E). It appears that the chimneys continue towards the seafloor as conduits considerably narrower compared to main underlying chimney conduits (Fig. 4, 6 and 7).

## **5. Discussion**

### **5.1 Understanding seismic truncations**

#### **Seismic resolution**

With a dominant frequency of 80 Hz. the recorded seismic signal has a vertical resolution ( $\lambda/4$ ) of 4.6-5 m within the upper 200 m in the sedimentary column. Because the 3D P-Cable data set has been 3D-migrated, the lateral resolution of the data is therefore equal to the bin size of 6 m. Buried relict carbonate domes or pockmarks of at least 5 m elevation difference and tens of meters width, typical dimensions of observed features at the present day Nyegga seafloor (e.g. Hovland and Svensen, 2006), can be well identified within the P-Cable 3D seismic data set.

Interruption of the continuity of sediment beds with a vertical thickness equal or higher than the vertical resolution would be distinguished in the seismic record as truncated reflections. Thinner truncated beds (< 5m) would not be resolved by the vertical resolution of the data set but they could be inferred by judging lateral changes in waveform and amplitude due to tuning effects caused by pinch-outs at the top of the buried features.

#### **Mechanisms explaining the truncations**

The truncation of seismic reflections described above may indicate sedimentation against dome-like features and/or sediment wash-out induced by the erosive character of dominant bottom currents at fluid vents on paleo-seafloors (Fig. 8). In the case of buried dome-like features, the seismic truncations and amplitude pinch-outs indicate the place where soft sediments overlapped the flanks of the dome until its burial (Fig. 8-E). In the case of

depression-like features (i.e. pockmarks) the truncations indicate the diameter of the area where sediments were washed-out during pockmark formation (Fig. 8-F).

Both mechanisms can explain the formation of truncated strata during chimney genesis in Nyegga, dominated by repetition of fluid expulsion phases and burial of associated methane vent-related features (Fig. 8). Initial stages of each fluid expulsion phase can be explained by the integration of three previously suggested mechanisms (Fig. 8): **(1)** sediment deformation by over-pressurised gas that escapes vigorously towards the seafloor (Fig. 8-A) at an early stage of chimney formation ; **(2)** chimney progression throughout fine grained sediments by generation of fracture networks (Jain and Juanes, 2009) and further emplacement of gas hydrates (Fig. 8-B) preferentially in veins and fractures (Plaza-Faverola et al., 2010b); and **(3)** precipitation of methane-derived authigenic carbonate (Fig. 8-C and E) within near seafloor sediments (Hovland and Svensen, 2006; Mazzini et al., 2006) as well as pockmark formation aided by bottom currents (Fig. 8-D and F) (e.g. Andresen et al., 2008; Boe et al., 1998; Hovland et al., 2002).

High fluid expulsion rates are inferred to decline to low rates after relatively short periods of substantial fluid depletion through chimneys (Hustoft et al., 2009). However, similar to pipes off-shore Namibia (Moss and Cartwright, 2010), the escape of hydrocarbons seemingly continues intermittently after the blow-out eventually developing seafloor expressions. The last stage of each activity phase is therefore dominated by micro-seepage of fluids. Depending on the local seep settings at different locations (i.e. mechanism of carbonate precipitation, fluid flow regime, influence of bottom currents and fluid venting duration) (e.g. Mazzini et al., 2006) pockmark-like or carbonate-dome like features formed (Fig. 8 E and F). Burial and therefore preservation of features at different depths (i.e. INT and H50 horizons) suggest that chimneys entered dormant periods in the interim between two active periods or have not been reactivated. Dormant periods are thought to be induced by self-sealing mechanisms following the emplacement of hard grounds within chimney conduits (Hovland, 2002; Naudts et al., 2010). Continuation of chimneys above truncated reflectors (Figs. 6-B, C, E and 7) indicates local re-generation of excess pore-pressure and seal by-passing. Brecciation of buried carbonate build-ups is expected as a result of bypassing over-pressurised fluids (Fig. 8-D).

Differences in the diameter of conduits within single chimneys may also indicate different periods of chimney activity. In general shallower conduits within a chimney are narrower than underlying conduits (Fig. 7-A). It is likely that for each new fluid escape period less

overpressure was required to bypass newly emplaced seals, leading to the formation of progressively narrower conduits associated to progressively younger periods of activity (Fig. 9).

### **Analogues of present day fluid expulsion-related features**

At Nyegga, both pockmarks and carbonate-mounds (e.g. Westbrook et al., 2008) have been observed and found to be often associated with authigenic carbonate precipitations (e.g. (Hovland et al., 2005; Mazzini et al., 2006). Nevertheless, their distribution seems to be randomly. We are not able to discern between the precise mechanism leading to one or the other type of structure. However, the observations and interpretations herein indicate that both type of structures may have been formed in the past and subsequently have been preserved by burial.

By simple analogy with the present day observations at venting systems in Nyegga the truncation of reflections against the chimney flanks observed at the depth of H50 and INT reflectors (Figs 5, 6, 7) may be explained by the mechanism suggested above (Fig. 8). Heights of observed truncated structures at the depth of INT and H50 reflectors (around 5 m according to seismic resolution) are within the range (3-10 m) of pockmarks and carbonate dome heights (Fig. 8 E and F) outcropping at the present day Nyegga seafloor (Hovland and Svensen, 2006; Hovland et al., 2005).

Moreover, contemporary methane-expulsion sites show very similar features as Nyegga's chimney systems. Naudts et al. (2010) describe up to 50 m high carbonate knolls and smaller carbonate mounds associated with active methane venting on the Hikurangi Margin, offshore New Zealand. These carbonates mounds may be modern analogues to the buried dome-like features reported in this study in the Nyegga area. Naudts et al. (2010) envision a model that describes differences in seep environment and among others explains the size of carbonate mounds at the top of seep conduits. Their model also nicely explains the observation of some of the truncations reported in this study (Fig. 8-E). Similarly, the 25 m high carbonate mound described by Riding et al., (2002) south of Belgium or the several meters high methane-derive authigenic carbonate (MDAC) chimneys reported at several fluid vents worldwide (e.g. Diaz-del-Rio et al., 2003; Judd and Hovland, 2007, pp. 299 and references therein) are also possible modern analogues of buried methane escape related features reported herein (Fig. 8).

Whether the truncations are associated with buried domes or associated with pockmarks, their occurrence provides indirect evidence of fluid escape in the past. The fact that truncations

occur at distinct but different depths indicates multiple but short-lived phases of active fluid escape in the Nyegga area.

## **5.2 Timing of chimney evolution and major fluid expulsion periods**

The well-established stratigraphic framework (Fig. 4) allows us to use seismic horizons, where truncations are observed, as chronological markers for former fluid venting periods. The stratigraphic observations and chimney classifications suggest that some Nyegga chimneys went through a multi-stage evolution with more than one phase of activity (fluid expulsion towards the seafloor).

### **Venting markers 160-200 ka and 125-130 ka.**

Most of the investigated chimneys present truncation of reflections only at the depth of the H50 reflector (Fig. 5-C, D). The H50 reflector (c. 160-200 ka.) is therefore likely to represent a main period of fluid expulsion and chimney formation in the Nyegga area (Fig. 9).

A few chimneys show truncations at the depth of the INT reflector (125-130 ka) in addition to the truncations above H50 (Fig. 5-A, B), indicating a second period of fluid expulsion and reactivation of chimneys (Fig. 9).

Considering a sedimentation rate of 0.5 m/ka (Hjelstuen et al., 2005) and a maximum thickness of truncated sediments of 5 m, the duration of these first fluid expulsion periods (160-200 ka and 125-130 ka) is inferred to be shorter than 10 ka. Indeed, depletion of overpressurised fluids through the chimneys is likely to happen only within a few years (Jain and Juanes, 2009).

The L50 unit (H50 and INT reflectors base and top respectively) is correlated to the Saalian glaciation (Figs 4, 9). Ploughmarks at the base and top of L50 unit suggest a proximity to the Saalian ice sheet and calving of large icebergs at the shelf edge during deglaciation (Dowdeswell and Bamber, 2007; Dowdeswell et al., 2007), i.e. last stage of the Saalian beginning of the interglacial (Fig. 4). Units L60 and L70, beneath L50 (Fig. 2), correlate to periods of reduced glaciations and/or free ice conditions (Fig. 9) where contour currents were efficient sediment transporters and contour drift deposition dominated (active thermohaline currents) (Gröger et al., 2003; Hohbein and Cartwright, 2006).

### **Youngest venting period**

Hustoft et al. (2009) suggested the LGM or shortly thereafter as major period of formation of Nyegga pockmarks due to fluid expulsion over a period of 3 ka. Non-truncated chimneys or chimneys that continue towards the seafloor beyond the truncated reflections (Fig. 5 and 6) are part of Hustoft et al. (2009) classification. Most of the truncated chimneys are likely to

have developed by two or three phases of fluid expulsions: an initial period of fluid expulsion and chimney formation at 160-200 ka; a second period of chimney formation and reactivation during the 125-130 ka time period; and second reactivation period after the LGM (Fig. 9-B). However, we cannot rule out that some of the chimneys reaching the seabed have only developed during the last phase of fluid expulsion following the LGM.

While considerable number of chimneys, understood as evident seismic blanking and pull-up reflections in the seismic data, have not reached the seafloor (Fig. 3), most of them connect to pockmarks or mounds at the present seafloor (Fig. 3-A). Many of them are associated with methane-vent related carbonate precipitations (Hovland and Svensen, 2006; Hovland et al., 2005; Mazzini et al., 2006). These observations support the dominance of micro-seepage (i.e. methane) at the last stage of each activity phase.

### **Possible older markers**

Although not as clearly seen as at the depth of H50 and INT reflectors, apparent truncation of reflections may be observed at the depth of the H70 reflector (Fig. 7-B). It is an intra Naust S reflector possibly correlated with MIS 10 of the Elsterian glaciation (Fig. 9-D). Older events of chimney formation in Nyegga (i.e.  $400 > ka > 300$ ) cannot thus be ruled out.

### **5.3 Fluid-escape periods triggered by glacial processes**

The occurrence of seismic markers (i.e. truncated reflections) that indicate more than one period of overpressure and chimney formation, coinciding with the last stages of major glacial cycles suggests that the glacial history of the region is crucial for understanding the factors triggering overpressure generation and chimney formation. Hustoft et al. (2009) have shown that rapid sediment loading due to glacially-derived sediments (i.e. GDFs) is a potential mechanism that could have driven fluid expulsion from previously over-pressured shallow gas reservoirs in Nyegga.

The contemporaneous occurrence of ploughmarks and truncated reflections, in the investigated Nyegga site, constitutes new evidence for relating focused fluid expulsion to overpressure generated by the emplacement of GDF sequences during the last three major glacial cycles (i.e. end of MIS 10, MIS 6 and MIS 2) (Fig. 9). During these three periods, but particularly during MIS 6 and MIS 2, the ice sheet has advanced to the shelf edge (Dahlgren et al., 2002). It is the only scenario in which we can expect iceberg scouring at the depth of paleo-seafloors in the Nyegga area. An ice sheet further inward on the shelf cannot create icebergs large enough to scour at depths beyond the shelf edge. Moreover, the emplacement of GDFs is related to an ice sheet that has pushed sediments across the shelf edge causing

them to be transported downslope. If the ice sheet itself and its effect on lithostatic pressure exerted an effect on the fluid expulsion is unclear, but given the proximity of the Nyegga area to the shelf edge, it cannot be ruled out.

The observations herein clearly suggest a link between fluid expulsion in the Nyegga area and maximum extent of the Fennoscandian ice sheet. The driving processes for fluid expulsion are very similar to those inferred for the history of sliding in the Storegga Slide complex (Bryn et al., 2005) and they also show a cyclicity, which can be related to the Pleistocene climatic fluctuations.

## 6. Conclusions

New high resolution P-Cable 3D seismic data is able to image focused fluid flow features in sedimentary basins, so-called chimneys, in much more detail than ever before. Chimneys that occur within the GHSZ in the Nyegga area of the mid-Norwegian margin show characteristic truncations of seismic reflections against the flanks and fronts of these structures but only at very particular depths. By analogy with present-day seafloor mounds and pockmarks, the observed truncated reflections may be explained by sedimentation against a buried positive structure (i.e. sediments deposited against the flanks of carbonate mounds) or by erosion related to the wash-out of sediment beds (i.e. process of pockmark formation). For that reason, the occurrence of truncated reflections is indicative of fluid expulsion at paleo-seafloors and represents a chronological marker for the timing of fluid flow activity.

Our observations support a formation scenario in which chimneys first formed by vigorous escape of over-pressurised fluids followed by continuous but low-flux fluid leakage before becoming dormant.

Nyegga chimneys are likely to have developed during one or several periods of activity. They can be classified at least in three major groups: **(1)** the youngest chimneys, with no stratigraphical evidence for several periods of reactivation. They formed as a single venting system most likely triggered by rapid sediment loading and overpressure build up after the LGM (18-25 ka); **(2)** Chimneys ca. 125-160 ka old, showing truncations mainly at H50 or INT reflectors, or at both levels, but terminating at the truncated event without any associated fluid flow expression at the present day seafloor; **(3)** Chimneys that have been reactivated one or two times during the last 200 ka and that have a fluid flow expression at the present seafloor.

The fluid-expulsion periods are seemingly related to the dynamic of the Fennoscandian Ice Sheet, i.e. to last stages of the Elsterian, Saalian and Weichselian glaciations. The



emplacement of thick sequences of glacial debris flow deposits during these maximum stages most likely caused rapid increase in overpressure and subsequently the formation of focused fluid flow features piercing through sediments of the Naust formation at Nyegga.

### **Acknowledgment**

The P-Cable 3D seismic data set was acquired on board R/V Jan Mayen, University of Tromsø, during a research cruise funded by the Norwegian Research Council PETROMAKS projects 169514/S30 and 175969/S30, and by the EU-funded HERMES project (GOCE-CT-2005-511234). We acknowledge the use of the P-Cable technology (Norwegian patent no. 317652) for the present investigation. We are thankful to the scientific and technical crew on board R/V Jan Mayen that helped during the acquisition of the 3D P-Cable seismic data. DECO Geophysical Moscow is acknowledged for processing of the data. We also would like to acknowledge Graham Westbrook for stimulating discussions on paleo-activity and for granting permission to include in the manuscript published 5 KHz profiler records. We are grateful to Mayte Pedrosa and Monica Winsborrow who provided constructive discussions on glacial processes.

## References

- Akhmetzhanov, A.M., Kenyon, N.H., Ivanov, M.K., Westbrook, G., and Mazzini, A., 2008, Deep-water depositional systems and cold seeps of the Western Mediterranean, Gulf of Cadiz and Norwegian continental margins. IOC Technical Series No. 76, UNESCO, 2008.
- Andresen, K.J., Huuse, M., and Clausen, O.R., 2008, Morphology and distribution of Oligocene and Miocene pockmarks in the Danish North Sea—implications for bottom current activity and fluid migration: *Basin Research*, v. 20, p. 445-466.
- Barber, A.J., Tjokrosapoetro, S., and Charlton, T.R., 1986, Mud volcanoes, shale diapirs, wrench faults, and melanges in accretionary complexes, eastern Indonesia: *AAPG Bull*, v. 70, p. 1729-1741.
- Berg, K., Solheim, A., and Bryn, P., 2005, The Pleistocene to recent geological development of the Ormen Lange area: *Marine and Petroleum Geology*, v. 22, p. 45-56.
- Boe, R., Rise, L., and Ottesen, D., 1998, Elongate depressions on the southern slope of the Norwegian Trench (Skagerrak): morphology and evolution: *Marine Geology*, v. 146, p. 191-203.
- Bryn, P., Berg, K., Stoker, M.S., Haflidason, H., and Solheim, A., 2005, Contourites and their relevance for mass wasting along the Mid-Norwegian Margin: *Marine and Petroleum Geology*, v. 22, p. 85-96.
- Bünz, S., Mienert, J., and Berndt, C., 2003, Geological controls on the Storegga gas-hydrate system of the mid-Norwegian continental margin: *Earth and Planetary Science Letters*, v. 209, p. 291-307.
- Bünz, S., Petersen, J., Iversen, S., Chand, S., Bialas, J., Rajan, A., Pless, G., Frantzen, J., Weibull, W., Poluboyarinov, M., Mandal, M., and Tiwari, A., 2008, Gas hydrates and fluid flow vents of the NBS-margin: Nyegga-northern flank of Storegga slide (P-cable 3D seismic acquisition, cruise report). *Petromaks-Gans and fluid flow project*. Tromsø-Tromsø, 13/07/08-26/07/08, R/V Jan Mayen.
- Cartwright, J., Huuse, M., and Aplin, A., 2007, Seal bypass systems: *AAPG bulletin*, v. 91, p. 1141.
- Cathles, L.M., Su, Z., and Chen, D., 2010, The physics of gas chimney and pockmark formation, with implications for assessment of seafloor hazards and gas sequestration: *Marine and Petroleum Geology*, v. 27, p. 82-91.

- Clark, J.I., Chari, T.R., Landva, J., and Woodworth-Lynas, C.M.T., 1989, Pipeline route selection in an iceberg-scoured seabed: *Marine Geotechnology*, v. 8, p. 51-67.
- Clennell, M.B., Hovland, M., Booth, J.S., Henry, P., and Winters, W.J., 1999, Formation of natural gas hydrates in marine sediments 1. Conceptual model of gas hydrate growth conditioned by host sediment properties: *Journal of Geophysical Research*, v. 104, p. 22985.
- Dahlgren, K.I.T., Vorren, T.O., and Laberg, J.S., 2002, Late Quaternary glacial development of the mid-Norwegian margin - 65 to 68 degrees N: *Marine and Petroleum Geology*, v. 19, p. 1089-1113.
- Diaz-del-Rio, V., Somoza, L., Martinez-Frias, J., Mata, M.P., Delgado, A., Hernandez-Molina, F.J., Lunar, R., Martin-Rubi, J.A., Maestro, A., Fernandez-Puga, M.C., Leon, R., Llave, E., Medialdea, T., and Vazquez, J.T., 2003, Vast fields of hydrocarbon-derived carbonate chimneys related to the accretionary wedge/olistostrome of the Gulf of Cadiz: *Marine Geology*, v. 195, p. 177-200.
- Dickens, G.R., 2002, Hydrocarbon-driven warming: *Nature*, v. 429, p. 513-515.
- Dowdeswell, J.A., and Bamber, J.L., 2007, Keel depths of modern Antarctic icebergs and implications for sea-floor scouring in the geological record: *Marine Geology*, v. 243, p. 120-131.
- Dowdeswell, J.A., Ottesen, D., Rise, L., and Craig, J., 2007, Identification and preservation of landforms diagnostic of past ice-sheet activity on continental shelves from three-dimensional seismic evidence: *Geology*, v. 35, p. 359-362.
- Foucher, J.P., Westbrook, G. K., Boetius, A., Ceramicola, S., Dupre, S., Mascle, J., Mienert, J., Pfannkuche, O., Pierre, C., Praeg, D., 2009, Structure and Drivers of Cold Seep Ecosystems: *Oceanography*, v. 22, p. 92-109.
- Gröger, M., Henrich, R., and Bickert, T., 2003, Glacial-interglacial variability in lower North Atlantic deep water: inference from silt grain-size analysis and carbonate preservation in the western equatorial Atlantic: *Marine Geology*, v. 201, p. 321-332.
- Hjelstuen, B.O., Eldholm, O., and Skogseid, J., 1999, Cenozoic evolution of the northern Voring margin: *Geological Society of America Bulletin*, v. 111, p. 1792-1807.
- Hjelstuen, B.O., Sejrup, H.P., Haflidason, H., Nygard, A., Ceramicola, S., and Bryn, P., 2005, Late Cenozoic glacial history and evolution of the Storegga Slide area and adjacent slide flank regions, Norwegian continental margin: *Marine and Petroleum Geology*, v. 22, p. 57-69.

- Hohbein, M., and Cartwright, J., 2006, 3D seismic analysis of the West Shetland Drift system: Implications for Late Neogene palaeoceanography of the NE Atlantic: *Marine Geology*, v. 230, p. 1-20.
- Hovland, M., 2002, On the self-sealing nature of marine seeps: *Continental Shelf Research*, v. 22, p. 2387-2394.
- Hovland, M., Gardner, J.V., and Judd, A.G., 2002, The significance of pockmarks to understanding fluid flow processes and geohazards: *Geofluids*, v. 2, p. 127-136.
- Hovland, M., and Judd, A.G., 1988, *Seabed Pockmarks and Seepages. Impact on Geology, Biology and the Marine Environment*. Graham & Trotman Ltd., London., 293 p.
- Hovland, M., and Svensen, H., 2006, Submarine pingoes: Indicators of shallow gas hydrates in a pockmark at Nyegga, Norwegian Sea: *Marine Geology*, v. 228, p. 15-23.
- Hovland, M., Svensen, H., Forsberg, C.F., Johansen, H., Fichler, C., Fossa, J.H., Jonsson, R., and Rueslatten, H., 2005, Complex pockmarks with carbonate-ridges off mid-Norway: Products of sediment degassing: *Marine Geology*, v. 218, p. 191-206.
- Hustoft, S., Bünz, S., and Mienert, J., 2010, Three-dimensional seismic analysis of the morphology and spatial distribution of chimneys beneath the Nyegga pockmark field, offshore mid-Norway: *Basin Research*, v. 22, p. 465-480.
- Hustoft, S., Dugan, B., and Mienert, J., 2009, Effects of rapid sedimentation on developing the Nyegga pockmark field: Constraints from hydrological modeling and 3-D seismic data, offshore mid-Norway: *Geochemistry Geophysics Geosystems*, v. 10, p. Q06012.
- Jain, A.K., and Juanes, R., 2009, Preferential Mode of gas invasion in sediments: Grain-scale mechanistic model of coupled multiphase fluid flow and sediment mechanics: *J. Geophys. Res.*, v. 114, B08101, doi: 10.1029/2008jb006002.
- Jansen, E., and Sjøholm, J., 1991, Reconstruction of glaciation over the past 6 Myr from ice-borne deposits in the Norwegian Sea: *Nature*, v. 349, p. 600-603.
- Jose, T., Minshull, T.A., Westbrook, G.K., Nouzé, H., Ker, S., Gailler, A., Exley, R., and Berndt, C., 2008, A Geophysical Study of a Pockmark in the Nyegga Region, Norwegian Sea. Proceedings of the 6th International Conference on Gas Hydrates (ICGH 2008), Vancouver, British Columbia, CANADA, July 6-10, 2008, 12pp. [<https://circle.ubc.ca/handle/2429/1022>].
- Judd, A.G., and Hovland, M., 2007, *Seabed fluid flow: the impact of geology, biology and the marine environment.*, Cambridge University Press, Cambridge, 475 p.

- Kennett, J.P., Cannariato, K.G., Hendy, I.L., and Behl, R.J., 2003, Methane Hydrates in Quaternary Climate Change: the Clathrate Gun Hypothesis, American Geophysical Union, Washington., 216 p.
- King, L.H., and Maclean, B., 1970, Pockmarks on Scotian Shelf: Geological Society of America Bulletin, v. 81, p. 3141-3148.
- Kopf, A., 1999, Fate of sediment during plate convergence at the Mediterranean Ridge accretionary complex: Volume balance of mud extrusion versus subduction and/or accretion: *Geology*, v. 27, p. 87.
- Kopf, A.J., 2002, Significance of mud volcanism: *Reviews of Geophysics*, v. 40, p. 1005.
- Kvenvolden, K.A., 1993, Gas hydrates—geological perspective and global change: *Rev. Geophys*, v. 31, p. 173–187.
- Leggett, J., 1990, The nature of the greenhouse threat, in *Global Warming, The Greenpeace Report*: New York, Oxford University Press, 14-43 p.
- Loseth, H., Gading, M., and Wensaas, L., 2009, Hydrocarbon leakage interpreted on seismic data: *Marine and Petroleum Geology*, v. 26, p. 1304-1319.
- Lygren, T.H., Berg, M.N., and Berg, K., 1997, *Sub-Glacial Features Interpreted from 3D-Seismic*: London, 60 p.
- MacDonald, G.J., 1990, Role of methane clathrates in past and future climates: *Climatic Change*, v. 16, p. 247-281.
- Mazzini, A., Svensen, H., Hovland, M., and Planke, S., 2006, Comparison and implications from strikingly different authigenic carbonates in a Nyegga complex pockmark, G11, Norwegian Sea: *Marine Geology*, v. 231, p. 89-102.
- Milkov, A.V., Claypool, G.E., Lee, Y.J., Xu, W., Dickens, G.R., and Borowski, W.S., 2003, In situ methane concentrations at Hydrate Ridge, offshore Oregon: New constraints on the global gas hydrate inventory from an active margin: *Geology*, v. 31, p. 833.
- Moss, J.L., and Cartwright, J., 2010, The spatial and temporal distribution of pipe formation, offshore Namibia: *Marine and Petroleum Geology*, v. 27, p. 1216-1234.
- Naehr, T.H., Eichhubl, P., Orphan, V.J., Hovland, M., Paull, C.K., Ussler, W., Lorenson, T.D., and Greene, H.G., 2007, Authigenic carbonate formation at hydrocarbon seeps in continental margin sediments: A comparative study: *Deep-Sea Research Part II-Topical Studies in Oceanography*, v. 54, p. 1268-1291.
- Naudts, L., Greinert, J., Poort, J., Belza, J., Vangampelaere, E., Boone, D., Linke, P., Henriët, J., and De Batist, M., 2010, Active venting sites on the gas-hydrate-bearing Hikurangi

- Margin, Off New Zealand: Diffusive-versus bubble-released methane: *Marine Geology*, v. 272, p. 233-250.
- Nisbet, E.G., 2002, Have sudden large releases of methane from geological reservoirs occurred since the Last Glacial Maximum, and could such releases occur again?: *Philosophical Transactions: Mathematical, Physical and Engineering Sciences*, v. 360, p. 581-607.
- Nisbet, E.G., and Chappellaz, J., 2009, Shifting gear, quickly: *Science*, v. 324, p. 477.
- Nygård, A., Sejrup, H.P., Haflidason, H., and Bryn, P., 2005, The glacial North Sea Fan, southern Norwegian Margin: architecture and evolution from the upper continental slope to the deep-sea basin: *Marine and Petroleum Geology*, v. 22, p. 71-84.
- Ottesen, D., Dowdeswell, J.A., and Rise, L., 2005, Submarine landforms and the reconstruction of fast-flowing ice streams within a large Quaternary ice sheet: The 2500-km-long Norwegian-Svalbard margin (57 degrees-80 degrees N): *Geological Society of America Bulletin*, v. 117, p. 1033-1050.
- Paull, C.K., Ussler, W., Holbrook, W.S., Hill, T.M., Keaten, R., Mienert, J., Haflidason, H., Johnson, J.E., Winters, W.J., and Lorenson, T.D., 2008, Origin of pockmarks and chimney structures on the flanks of the Storegga Slide, offshore Norway: *Geo-Marine Letters*, v. 28, p. 43-51.
- Petersen, C.J., Bünz, S., Hustoft, S., Mienert, J., and Klaeschen, D., 2010, High-resolution P-Cable 3D seismic imaging of gas chimney structures in gas hydrated sediments of an Arctic sediment drift: *Marine and Petroleum Geology*, v. doi: 10.1016/j.marpetgeo.2010.06.006, p. 1-14.
- Planke, S., and Berndt, C., 2003, Apparatus for seismic measurements, Norwegian patent no. 317652.
- Plaza-Faverola, A., Bünz, S., and Mienert, J., 2010a, Fluid distributions inferred from P-wave velocity and reflection seismic amplitude anomalies beneath the Nyegga pockmark field of the mid-Norwegian margin: *Marine and Petroleum Geology*, v. 27, p. 46-60.
- Plaza-Faverola, A., Westbrook, G.K., Ker, S., Exley, R., Gailler, A., Minshull, T.A., and Broto, K., 2010b, Evidence from 3D seismic tomography for a substantial accumulation of gas hydrate in a fluid-escape chimney in the Nyegga pockmark field, offshore Norway: *J. Geophys. Res.*, v. doi:10.1029/2009JB007078, in press.

- Polyak, L., Edwards, M.H., Coakley, B.J., and Jakobsson, M., 2001, Ice shelves in the Pleistocene Arctic Ocean inferred from glaciogenic deep-sea bedforms: *Nature*, v. 410, p. 453-457.
- Riding, R., 2002, Structure and composition of organic reefs and carbonate mud mounds: concepts and categories: *Earth-Science Reviews*, v. 58, p. 163-231.
- Rise, L., Ottesen, D., Berg, K., and Lundin, E., 2005, Large-scale development of the mid-Norwegian margin during the last 3 million years: *Marine and Petroleum Geology*, v. 22, p. 33-44.
- Rise, L., Ottesen, D., Longva, O., Solheim, A., Andersen, E.S., and Ayers, S., 2006, The Sklinnadjupet slide and its relation to the Elsterian glaciation on the mid-Norwegian margin: *Marine and Petroleum Geology*, v. 23, p. 569-583.
- Rise, L., Sættem, J., Fanavoll, S., Thorsnes, T., Ottesen, D., and Bøe, R., 1999, Sea-bed pockmarks related to fluid migration from Mesozoic bedrock strata in the Skagerrak offshore Norway: *Marine and Petroleum Geology*, v. 16, p. 619-631.
- Sejrup, H.P., Haflidason, H., Hjelstuen, B.I., Nygard, A., Bryn, P., and Lien, R., 2004, Pleistocene development of the SE Nordic seas margin: *Marine Geology*, v. 213, p. 169-200.
- Skene, K.I., Piper, D.J.W., Aksu, A.E., and Syvitski, J.P.M., 1998, Evaluation of the global oxygen isotope curve as a proxy for Quaternary sea level by modeling of delta progradation: *Journal of Sedimentary Research*, v. 68, p. 1077.
- Vaular, E.N., Barth, T., and Haflidason, H., 2010, The geochemical characteristics of the hydrate-bound gases from the Nyegga pockmark field, Norwegian Sea: *Organic Geochemistry*, v. 41, p. 437-444.
- Wadhams, P., 2000, *Ice in the Ocean*: London, Gordon and Breach Science Publishers, 335 p.
- Westbrook, G.K., Exley, R., Minshull, T.A., Nouzé, H., Gailler, A., Jose, T., Ker, S., and Plaza, A., 2008, High-resolution 3D seismic investigations of hydrate-bearing fluid-escape chimneys in the Nyegga region of the Vøring plateau, Norway, *Proceedings of the 6th International Conference on Gas Hydrates (ICGH 2008)*, Vancouver, British Columbia, CANADA, July 6-10, 2008, 12pp.  
[<https://circle.ubc.ca/handle/2429/1022>].
- Xu, W., and Ruppel, C., 1999, Predicting the occurrence, distribution, and evolution of methane gas hydrate in porous marine sediments: *Journal of Geophysical Research-Solid Earth*, v. 104, p. 5081-5095.









Chimney types	Type description	
a 	Truncation and termination above H50 reflector.	Truncated chimneys
b 	Truncation at H50 and/or at INT reflector, termination of chimney before the seafloor, pockmark associated.	
c 	Truncation at H50 reflector but can be related to ploughmark flanks, termination of chimney before the seafloor, some has expression at the seabed.	
d 	Truncation above H50 and INT reflectors, termination above INT reflector.	
e 	Truncation above INT and/or H50 reflector, termination of the chimney at INT but with seafloor expression.	
f 	No truncations, terminate at H50 reflector but may have a seafloor expression.	Non-truncated chimneys
g 	No truncation, terminate before the seafloor, no clear seafloor expression, some are very narrow.	
h 	No truncation, terminate before the seafloor, has a well define seafloor expression, some are very narrow.	

Table 1: Classification of truncated and non-truncated chimneys. Each type (a-h) is shortly described. Associated symbols are used for location of some of the examples in Fig. 5-C.



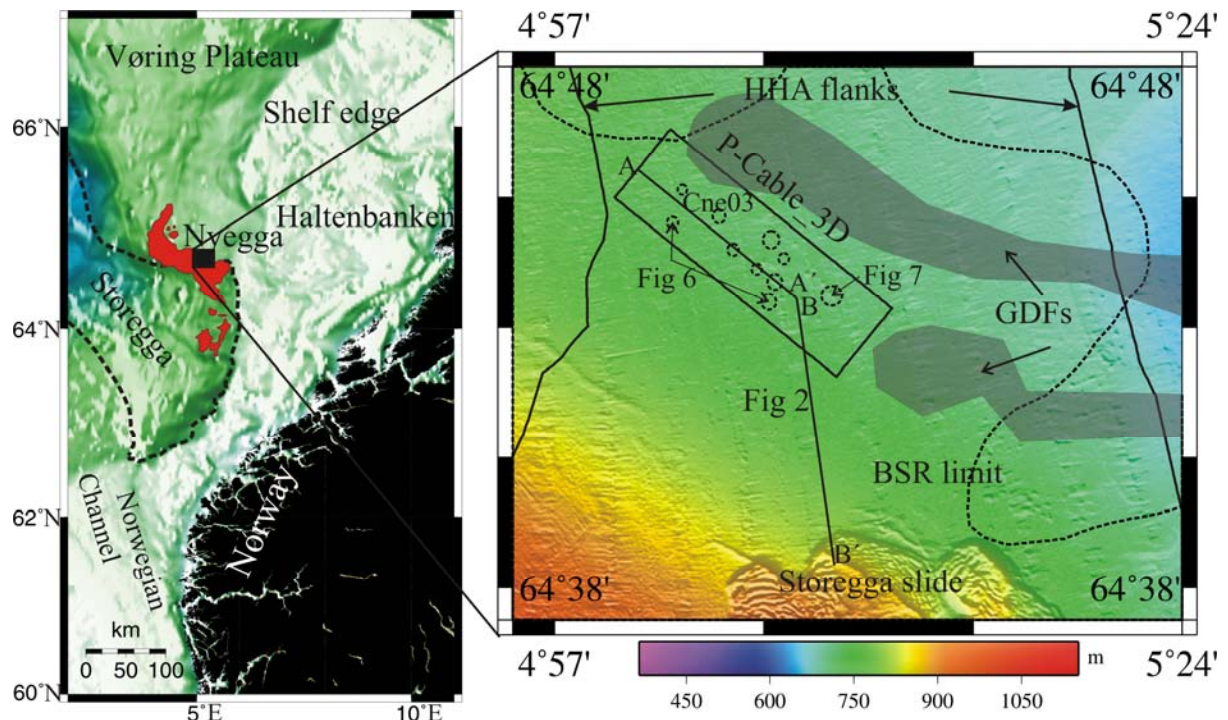


Fig. 1: Location map of Nyegga respect to the Norwegian continental shelf edge, Storegga slide and bordering regions. The BSR map of the region (Bünz et al., 2003) is included. The inset shows the area covered by the high resolution P-cable 3D data set and investigated chimneys (Fig. 6 and 7). Schematic representation of buried glacigenic debris flows reaching the investigated area is included in light grey (inset).

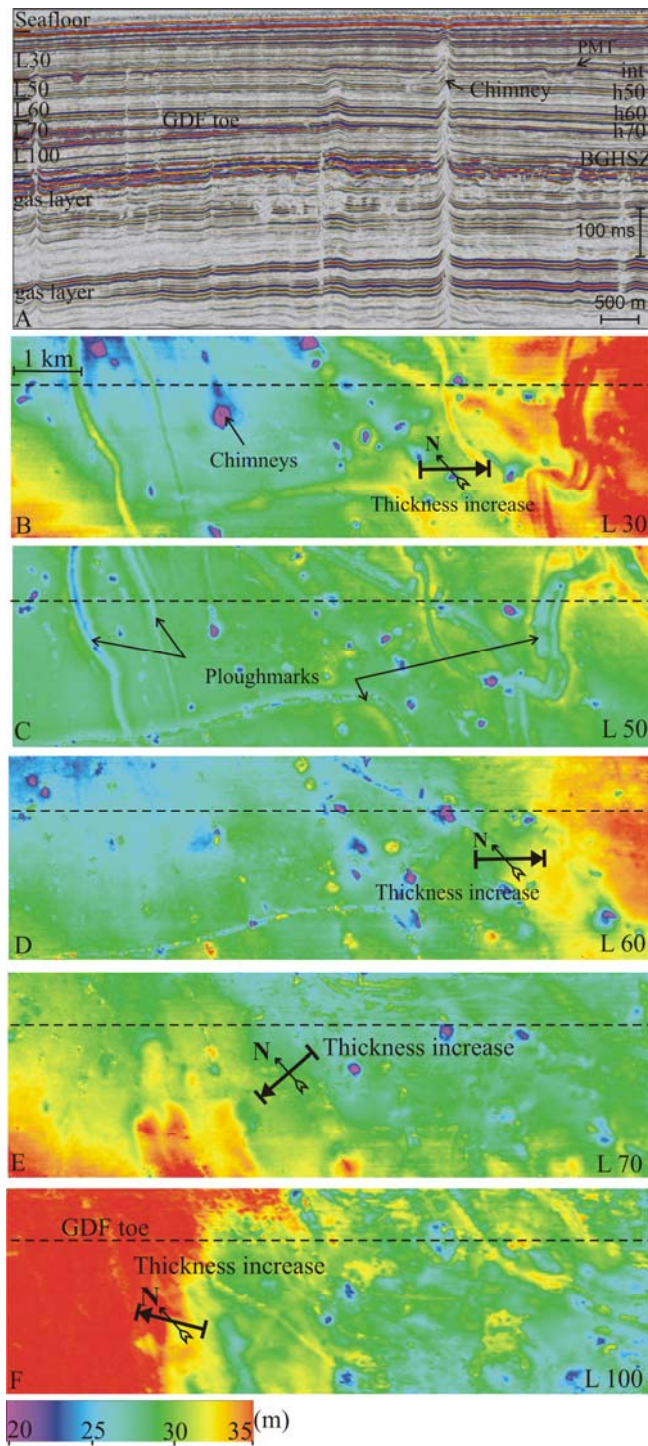


Fig. 2: Thickness maps for units L30 (B), L50 (C), L60 (D), L70 (E) and L100 (F), indicated in the seismic profile (A). The thickness scale is set to cover a range of 15 m for each unit. Interval velocities used for depth conversion are, from top to bottom: 1500, 1500, 1590, 1680, 1890 m/s (Plaza-Faverola et al., 2010b). PMT stands for ploughmark truncations, GDF for glaciogenic debris flow. The dashed line indicates the location of the seismic profile (A) in the maps (B-F). The arrows point towards regions of maximum thickness increase.



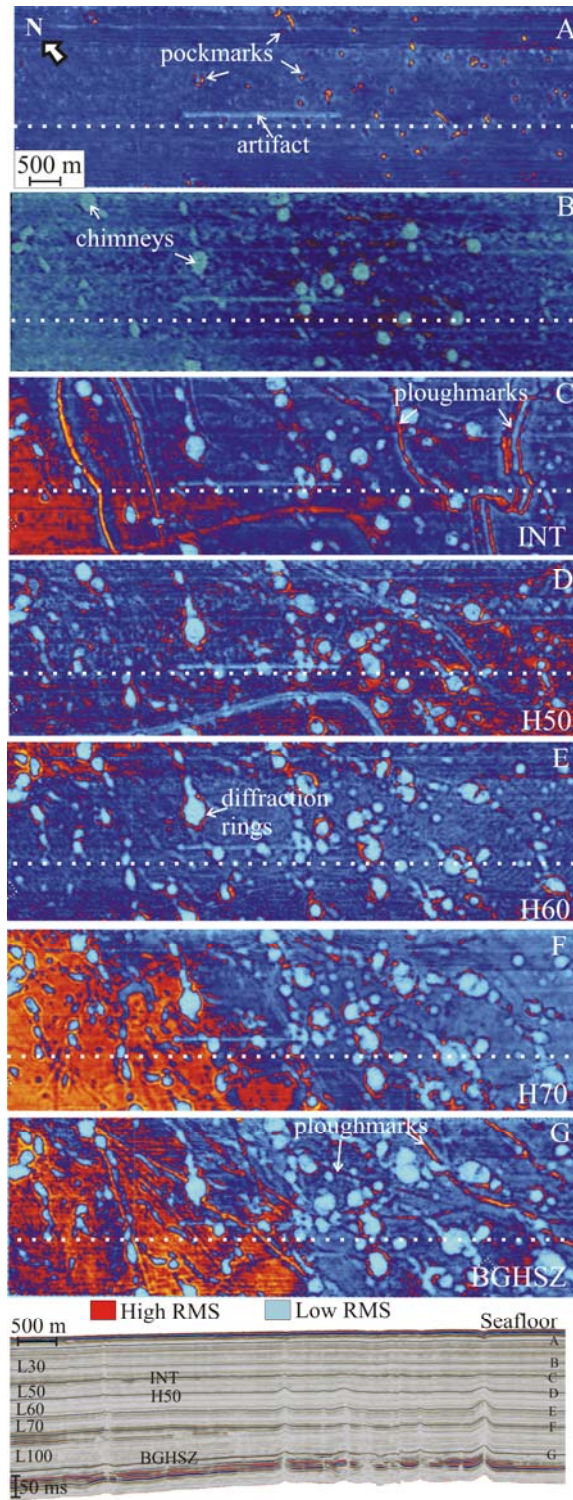


Fig. 3: RMS amplitude maps (A-G) from the non-migrated 3D P-Cable data set, within a time window of 10-15 ms centred at the reflectors indicated in the seismic section (bottom). Chimneys appear as circular features with the lowest RMS values (light blue).

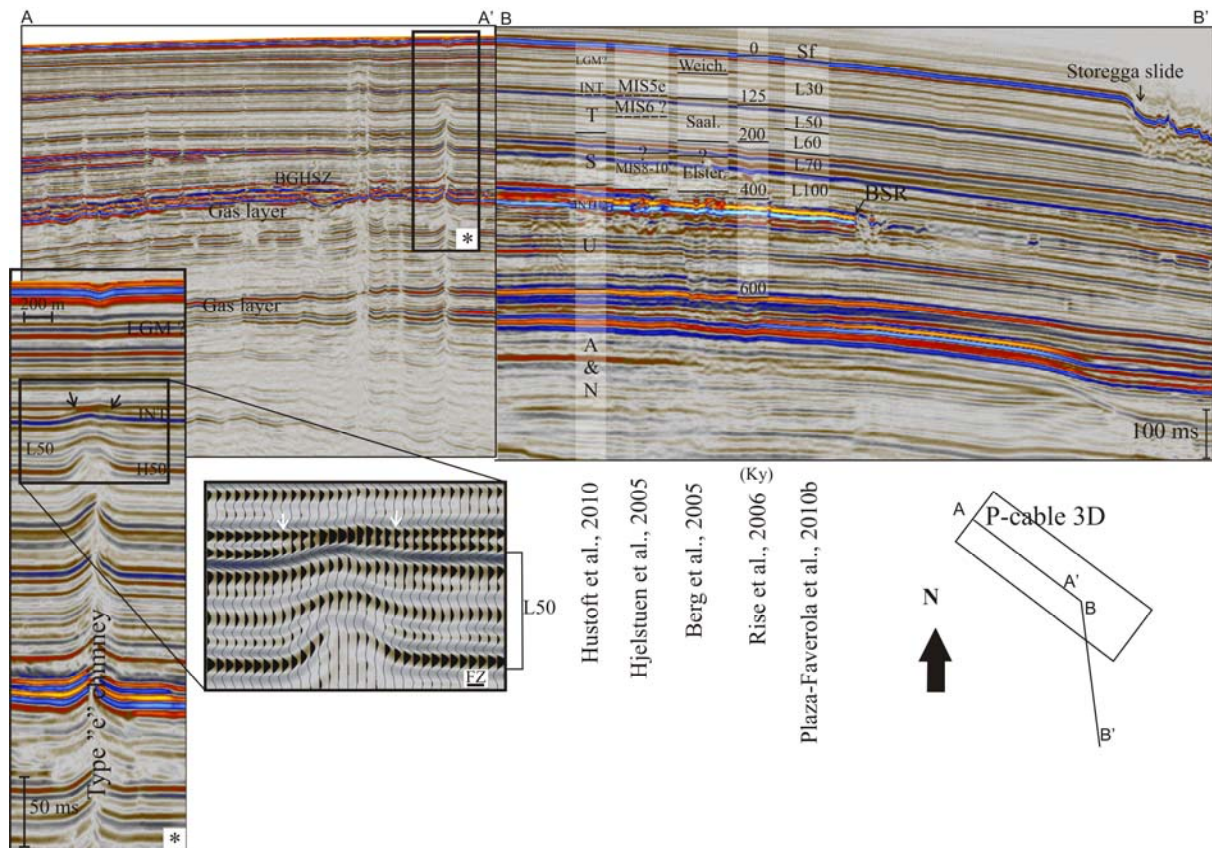


Fig. 4: Stratigraphical correlation cross-cutting a SE-NW profile from the P-cable 3D data set with a profile running parallel to the N-S profile in Fig. 5 by Hustoft et al., (2010) (see Fig. 1 for location). Relevant age information and correlation with pre-established intra-Naust units in Nyegga and nearby areas, is included. The inset (\*) shows the main reflectors (INT and H50) where depositional patterns within chimneys are investigated herein.



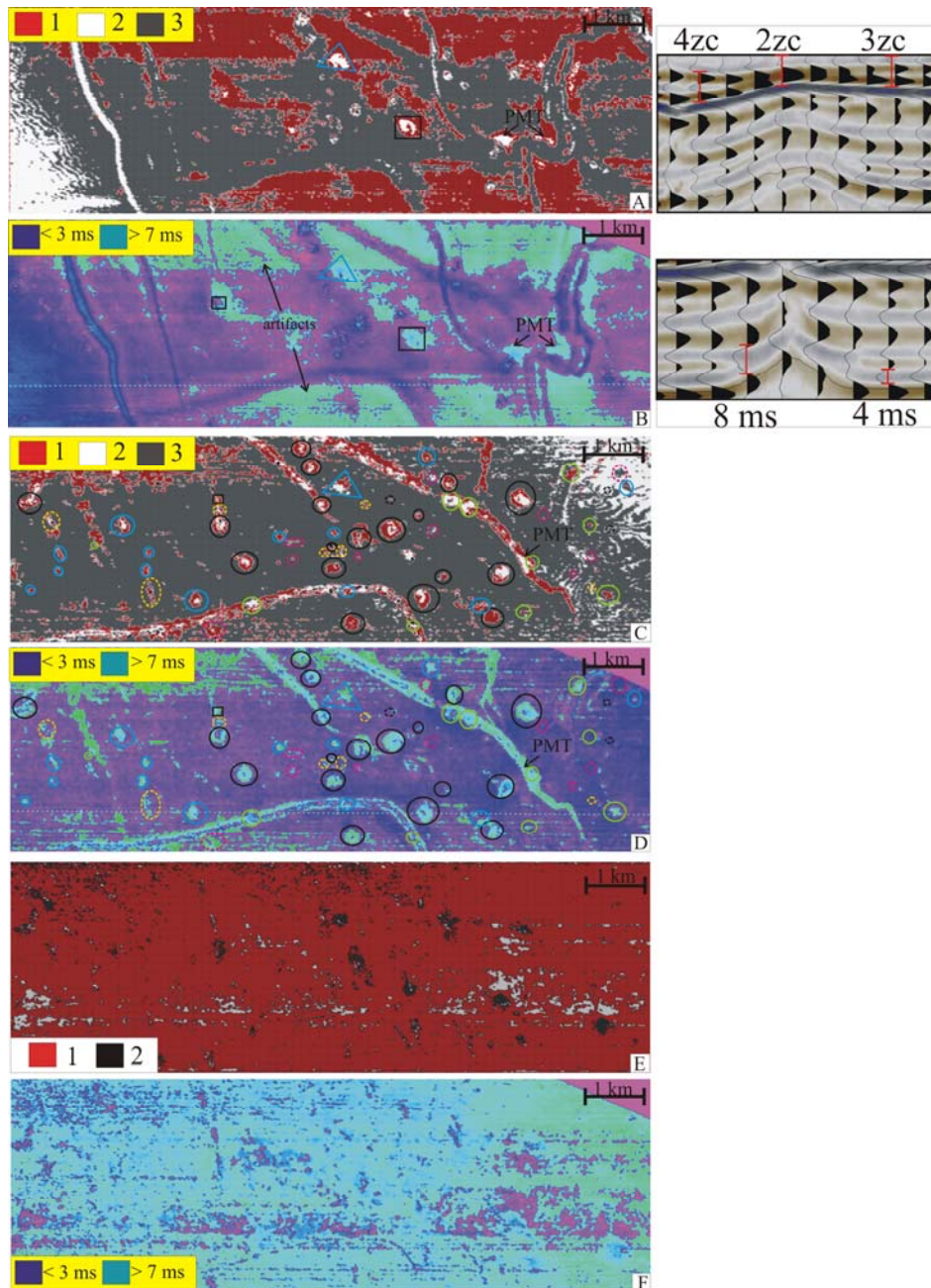


Fig. 5: Zero crossing and loop duration maps of the two major horizons where truncations are observed: INT (A and B) and H50 (C and D). Similar maps of H60 horizon (E and F) show how the maps look in horizons where no truncations are observed. See Fig. 3-A for location of the horizons. The scales in A, C and E represent the number of zero “amplitude” crossing within a window of 12 ms above the respective reflectors (inset in map A). Truncations are indicated by a jump from 3 to 1 in the number of mapped zero-crossing. The scales in B, D and F represent the time length of the seismic signal loop within a time window (inset in map B). PMT stands for ploughmark truncation.

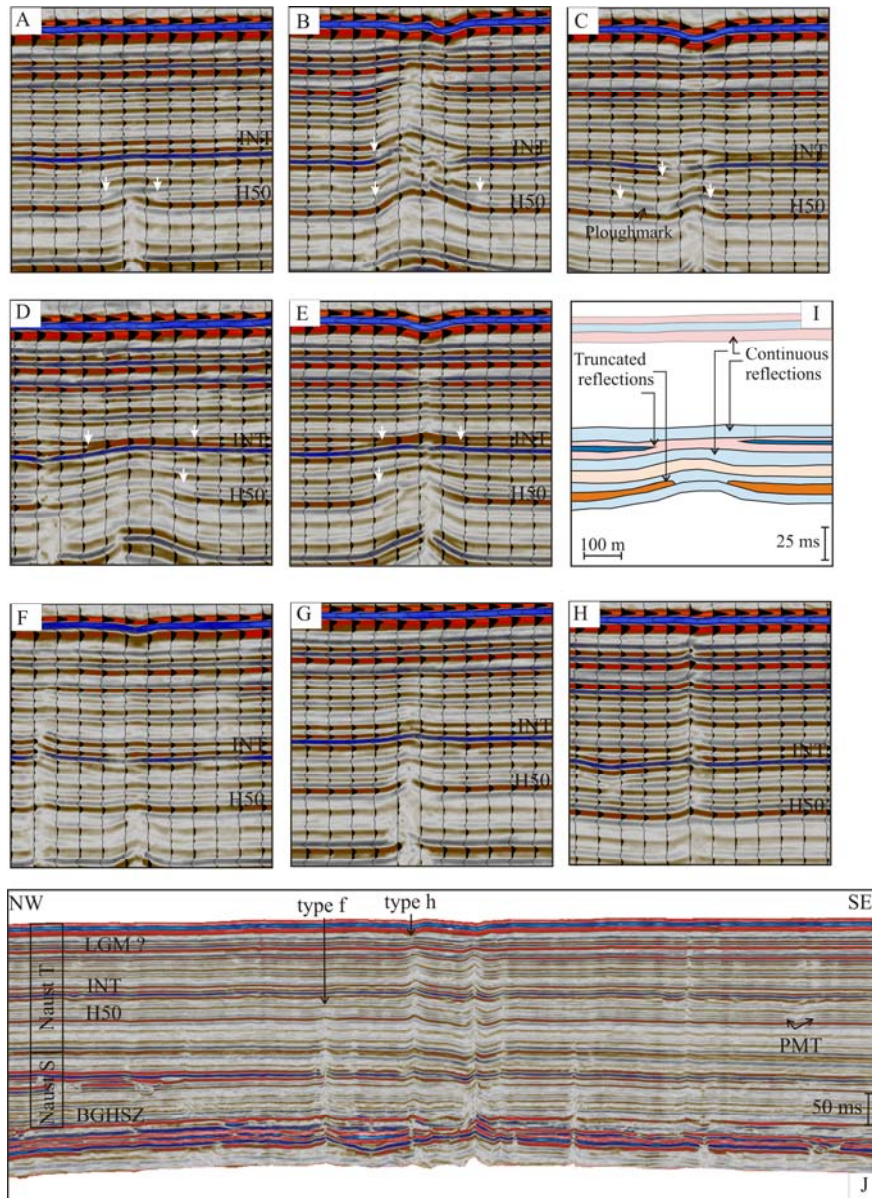


Fig. 6: Seismic character of truncated chimneys (panels A-E) classified as type a-e and of non-truncated chimneys classified as type f-h (panels F-H) in table 1. Small white arrows denote truncated reflections. A schematic comparison of truncated and continuous reflections is shown in panel I. Examples of type f and h chimneys are included in the seismic section (J) to show the difference related to the termination of chimneys at the depth of truncated reflections or closer to the present-day seafloor.



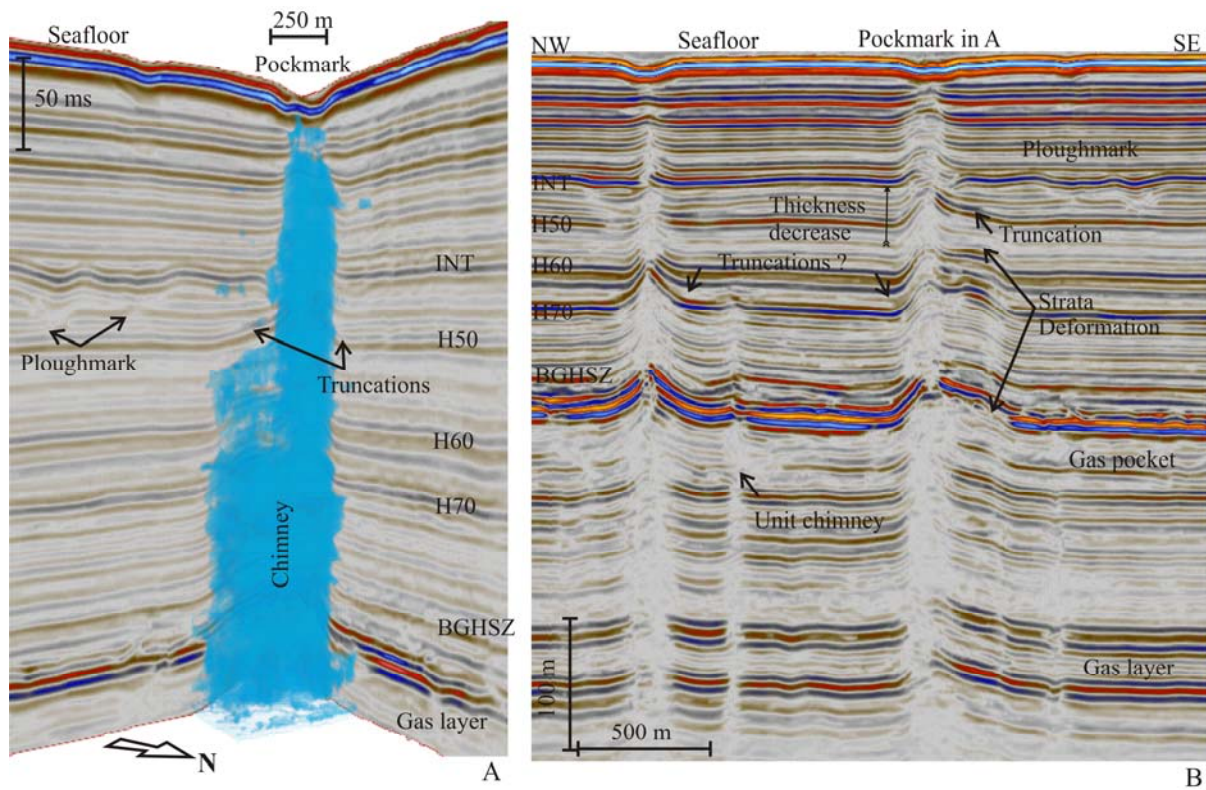


Fig. 7: (A) Isolation of a type “b” chimney (see fig. 1 for location) based on the correlation between RMS and variance attributes. Chimneys are characterized by anomalous low amplitudes and high variance values at their interiors. (B) Seismic depth converted section showing the same chimney in (A) but seen from the south. Depth conversion uses  $V_p$  interval velocities from Plaza-Faverola et al., (2010b). A decrease in chimney diameter is evident at the H50 reflector.

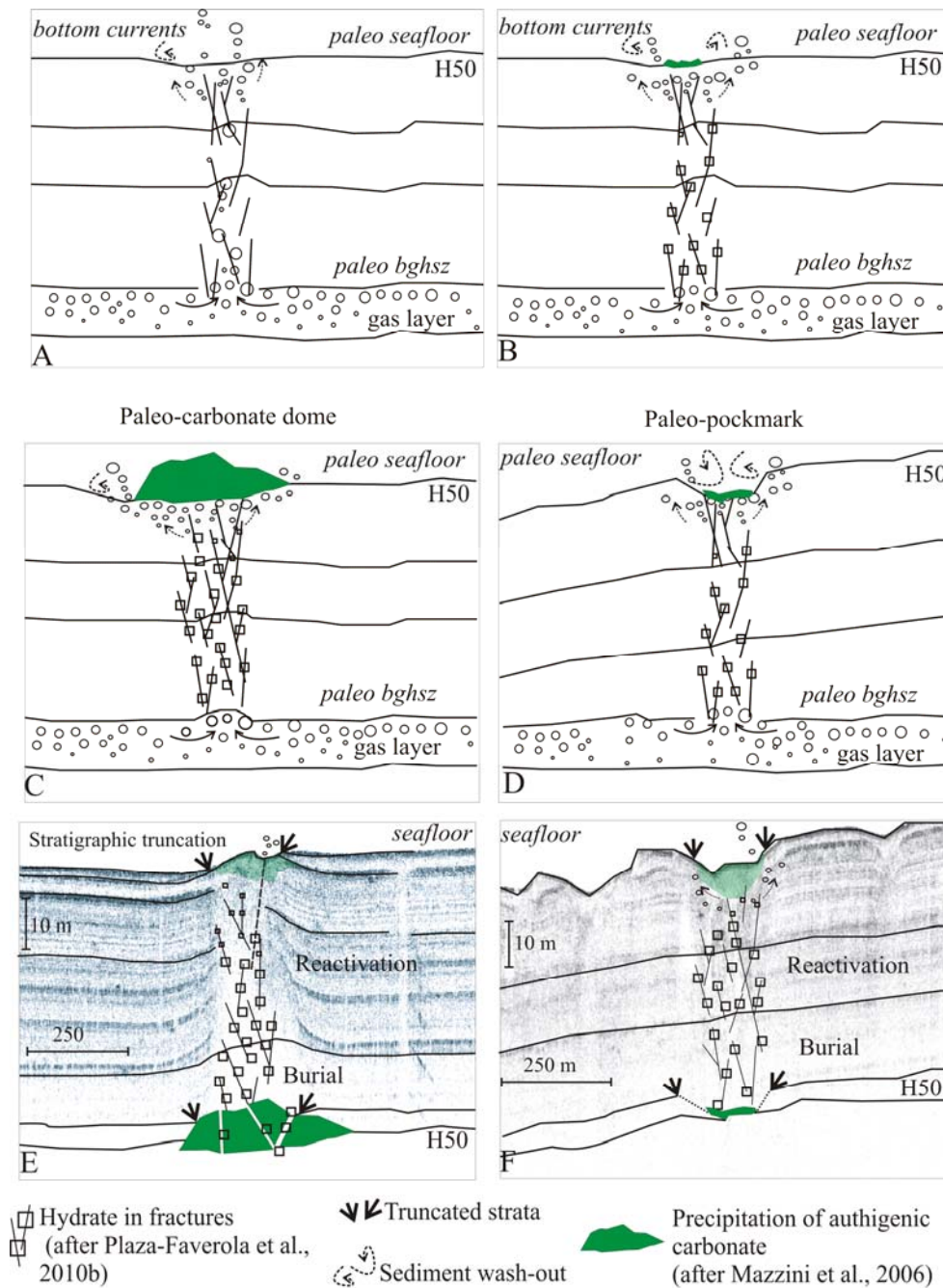


Fig. 8: Schematic representation of the mechanisms explaining seismic truncations at paleo seafloors in Nyegga. See text for detailed explanation. The representation of authigenic carbonate precipitation is extracted from Mazzini et al., (2006) and hydrate emplacement in fractures from Plaza-Faverola et al., 2010b. The 5 kHz profiler images (E and F) has been modified from Westbrook et al., (2008) and were acquired during TTR 16-leg 3.



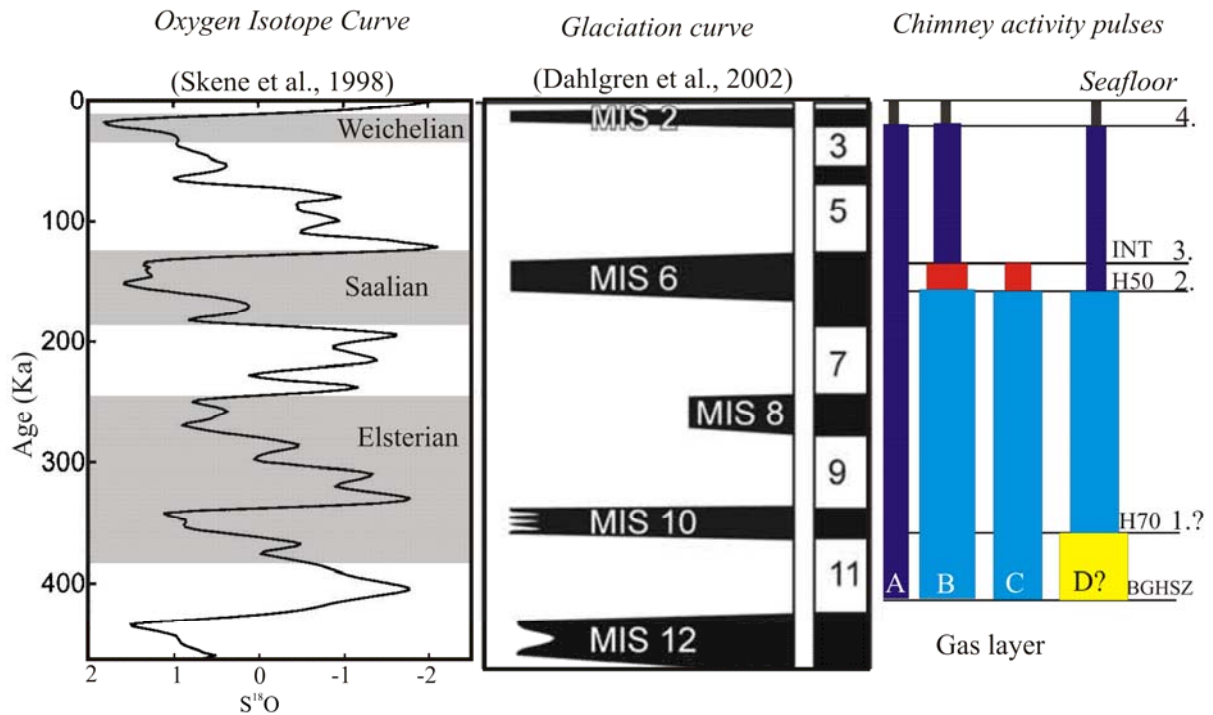


Fig. 9: Time-scale of main inferred periods of chimney formation and re-activation in Nyegga correlated to oxygen isotope curve (Skene et al., 1998) and glaciations curve (Dahlgren et al., 2002) of the region. A main venting cycle (2) is suggested at 160-200 ka, coinciding with the last stage of the Saalian glaciation. Some of the chimneys were reactivated at 125-130 ka (3). The youngest chimneys and reactivation is believed to postdate the LGM (4) (Hustoft et al., 2009). A possible older period (D) of fluid expulsion may date from early Elsterian glaciations (1). The youngest chimneys (A) formed during period 4. Most of the chimneys formed in 2, where reactivated in 3 and in 4 (B). Some chimneys were not reactivated in 4 (C).